Insertion Loss Spectrums Behind Straight Noise Barriers: Scaled Experiments

P. Bhuripanyo[1, *], S.I. Voropayev[2, 3] and H.J.S. Fernando[2]
[1]International School of Engineering, Chulalongkorn University, Bangkok, 10330, Thailand
[2]University of Notre Dame, Notre Dame, Indiana 46556, USA
[3]P.P. Shirshov Institute of Oceanology, Russian Academy of Sciences, Moscow 117851, Russia
[*]Corresponding author

***Abstract*—The results of scaled acoustic laboratory experiments with noise barriers are reported. Short impulsive spherical sound wave with broad frequency spectrum is used as controllable sound source. Using spectral analysis the insertion loss spectral functions were calculated for experiments with different source-receiver positions. The results were rescaled to traffic barriers and for typical traffic noise spectrum the values of the traffic barrier efficiency (a single number rating) were estimated and the directivity diagrams obtained.**

Keywords-sound barriers; diffraction from top; impulsive "point" sound source; barrier efficiency

I. INTRODUCTION

Noise barriers are broadly used to reduce noise in the vicinity of roads. In the presence of a barrier, noise at a receiver location from a source is due to transmitted pathway through the barrier and diffracted waves at the top of a barrier. Barriers are usually built with solid materials and effectively block direct sound propagation. Thus, the barrier performance is limited by the diffracted sound which is highly dependent on the source frequency, relative source and receiver positions and geometry of the barrier top [1]. Recently a comprehensive experimental study with different barrier tops (T-, L-shape, jagged regular and random, etc.) was conducted in "unpublished" [2]. We do not repeat this material and only results related to the straight tops, which are not included in [2], are reported below.

Traffic barriers are costly (about $1 million per kilometer) and knowledge of their efficiency is important. Usually the shielding effect of the barrier is quantified by the insertion loss which is a measure of the sound attenuation due to the presence of the barrier. The insertion loss may be defined as (e.g., [3])

$$IL = 10\log_{10}(P_0 / P)^2 \qquad (1)$$

where P_0, P are the RMS sound pressure without and with the barrier.

At present, only insertion loss for the case of the straight top is parameterized in terms of the Fresnel number, *Fn,* (Figure 1)

$$Fn = F_0 \cos\beta, \quad F_0 = 2(a+b-c)/\lambda = 2f\delta/C \qquad (2)$$

where $\delta=(a+b-c)$, C is the speed of sound, f is the sound frequency, $\lambda=C/f$ is the sound wave length.

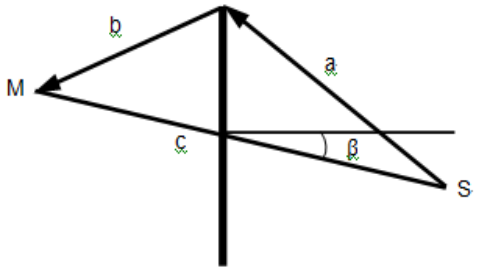

FIGURE I. BARRIER (SOLID VERTICAL LINE) AND SOUND SOURCE (S) AND MICROPHONE (M) GEOMETRY.

Basing on the experiments reported in [4], the following broadly used empirical parameterization for the insertion loss (in dB) was proposed [5]

$$IL = a + 20\log_{10}\frac{\sqrt{2\pi Fn}}{\tanh\sqrt{2\pi Fn}} \qquad (3)$$

where a is an empirical constant (the results of our experiments, see below, give a=6.5 and this value is used for estimates).

The experimental data reported in [4], were obtained for different wave lengths, λ, by using the source with different monofrequencies. Thus, the insertion loss, at particular value of δ in (2), was obtained only for specific frequency used. In our approach, short impulsive spherical sound wave with broad frequency spectrum is used as controllable sound source. This permits, by using the spectral analysis, to calculate for each value of δ used the insertion loss spectral functions for the whole frequency band, thus much more data are available. Because the frequency range of the laboratory sound source (5–30 kHz) is 10 times the frequency of the traffic noise (500–3000 Hz), the experiments can be considered as a 1:10 scaled experiments of a real traffic noise barrier.

II. EXPERIMENTAL SET-UP AND METHOD

Details of the experimental set-up and methods are similar to that used in [2] and only brief description is given below. Custom build 3-electrode spark discharger was used as a sound

© 2015. The authors - Published by Atlantis Press

source. For short sound pulse the primary signal diffracts above the barrier and arrives to the receiver earlier than the secondary (reflected/diffracted from surroundings) signal. The latter is ignored and only the information from the primary signal is used thus eliminating the need to use expensive acoustic anechoic chambers. The sound pressure was measured by the Brüel & Kjær 1/4" free-field microphone with preamplifier, TEDS, and microphone conditioning amplifier. Tektronix 100 MHz digital storage oscilloscope was used to digitize the pressure signal and store it into computer with the LabVIEW software. After each experiment the measured signals were post processed using the custom built MATLAB software.

Methods of spectral analyses were used in the data processing. First, the pressure frequency spectrums were calculated from the initial sound pressure time, *t*, traces and then the insertion losses *IL* were calculate as functions of frequency, *f*, and source-microphone position

$$IL = 10\log_{10}\left|S_0(f)/S_S(f)\right|^2 \tag{4}$$

where, S_0 is the spectral density amplitude for the free signal and S_S for the case of the barrier. Two different methods were used to calculate frequency spectrums, namely, standard fast Fourier transform (FFT) and the 1/3 Octave filter developed in "unpublished" [6].

As follows from (4), the insertion loss function gives the relative sound attenuations for different frequencies and these attenuations do not depend directly on the sound source used in the measurements. This permits the use in experiments of short sound pulses with advantages mentioned above.

The main idea of the scaled experiments is to measure insertion loss functions in relatively small laboratory experiments with high sound frequency and recalculate the results to real noise barriers. In our experiments the frequency range of the sound source is 10 times the frequency of traffic noise and the experiments can be considered as a 1:10 scaled experiments. The frequency of the measured in laboratory insertion loss function is simply rescaled from the laboratory frequency *f* to the traffic noise frequency *F* as *F=f*/10. Then, using rescaled insertion loss function and proper estimates for the free traffic noise spectrum, the characteristics of the diffracted traffic noise behind a barrier can be estimated. In particular, averaged over the traffic noise frequency range the barrier efficiency, or the so called single number rating (see below), can be calculated and compared for different conditions.

Because the sound pressure of the diffracted signal, *P,* is a function of many parameters, $P=P(t, R, \theta_S, \theta_m)$, the spectral density amplitude and the insertion loss are also functions of similar parameters

$$IL = IL(f, R, \theta_S, \theta_M) \tag{5}$$

where R, θ_S, θ_m describe the geometry of measurements (Figure 2).

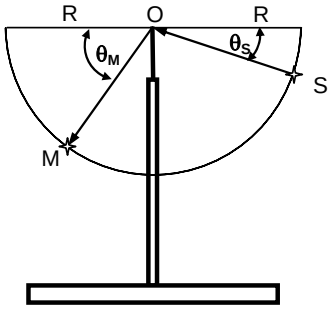

FIGURE II. SCHEMATIC SHOWING MICROPHONE, M, SOUND SOURCE, S, AND ANGLES, Θ, RELATIVE TO THE HORIZONTAL LINE PASSING THROUGH THE ORIGIN, O, WHICH COINCIDES WITH THE TOP OF THE BARRIER.

In experiments the microphone and the sound source were at the same distance, *R*=30 or 45 cm, from the origin and angles used are: θ_S=15, 30 degrees, θ_M = 0, 15, 30, 45 degrees. In total 16 sets of experiments were conducted. The following notation is used below for different geometries, e.g., S30M15R30 means θ_S=30, θ_M=15 degrees, R=30 cm. Note that for traffic barriers the frequency and length scale are rescaled as 1:10.

III. RESULTS

Figure 3 shows insertion loss, IL, as a function of the traffic frequency, *F*, for the S30M00R30 geometry of measurements. The results of the FFT calculations are shown on the top graph, the results of the 1/3 Octave filter calculations are shown on the bottom graph. For comparison, the dashed line shows the estimate (3). Both FFT and 1/3 Octave filter methods are in a satisfactory agreement. Some variability in the FFT data at high frequencies is related to the constant spectral window width, 100 Hz, which becomes small at high frequencies and the resulting "noise" is noticeable. In the 1/3 Octave filter calculations the window width is proportional to the central filter frequency and increases with the frequency and there is no such "noise". For comparison, the dashed line in these graphs shows the estimate (3) and agreement with both FFT and 1/3 Octave filter calculations is satisfactory.

Similar results were obtained for all other experiments. The example showing the insertion loss, IL, as a function of the traffic frequency, *F*, for S30M00R45 (top) and S30M45R30 (bottom) geometries are given in Figure 4. Only 1/3 Octave filter calculations are shown. Again, comparison with (3) shows satisfactory agreement.

All data for the insertion loss measurements are summarized in Figure 5. In this figure the ratio, $A=IL_{EXP}/IL_{EST}$, between the experimentally measured insertion losses, IL_{EXP}, and values, IL_{EST}, estimated from (3) are shown as a function of the traffic frequency, *F,* for all experiments conducted. In each graph eight points at each 1/3 Octave central frequencies show the results of measurements at eight different source-receiver angles. In the range of medium frequencies, which are the most important in a traffic noise, the standard deviation is about ±1.0 dB. Thus (3) with a=6.5 rather accurately approximates the measured insertion loss spectrums for different geometries of measurements.

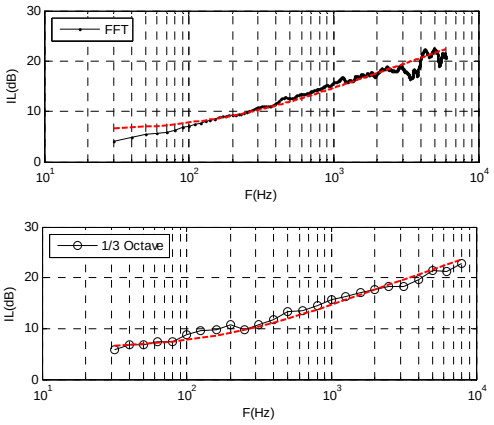

FIGURE III. IINSERTION LOSS, IL, AS A FUNCTION OF THE TRAFFIC FREQUENCY, F=F/10. TOP - FFT, BOTTOM – 1/3 OCTAVE FILTER CALCULATIONS. DASHED LINE - THE ESTIMATE (6). GEOMETRY OF MEASUREMENTS – S30M00R30.

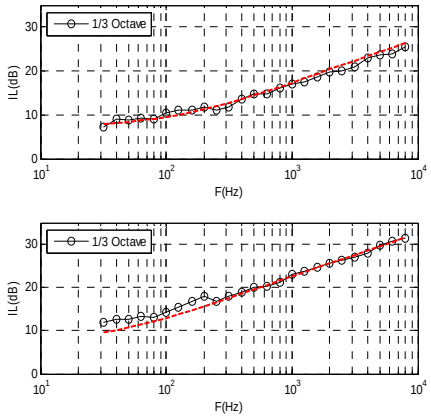

FIGURE IV. INSERTION LOSS, IL, AS A FUNCTION OF THE TRAFFIC FREQUENCY, F=F/10, 1/3 OCTAVE FILTER CALCULATIONS. GEOMETRY OF MEASUREMENTS: S30M00R45 (TOP), S30M45R30 (BOTTOM). DASHED LINE - THE ESTIMATE (6).

Using detailed data on the insertion loss spectrums, the single number insertion loss N for traffic barrier was estimated as follows. The insertion loss spectrum, IL(f), as measured in experiments, is rescaled from the laboratory, f, to the field, F=f/10, frequencies as

$$IL(F) = IL(f/10) \tag{6}$$

Some proper empirical or analytical parameterization for the traffic nose spectrum, $S_0(F)$, is used with correction, $S_A(F)$, on the standard A-weighting factor. In the estimates below we used for $S_0(F)$ the parameterization [7]

$$S_0(F) = -10log_{10}\left[1+(F/2000)^2\right] \tag{7}$$

This gives for the corrected traffic noise spectrum the estimate

$$S(F) = -10log_{10}\left[1+(F/2000)^2\right] + S_A(F) \tag{8}$$

where $S_A(F)$ is the standard A-weighting value for 1/3 octave band with center frequency F.

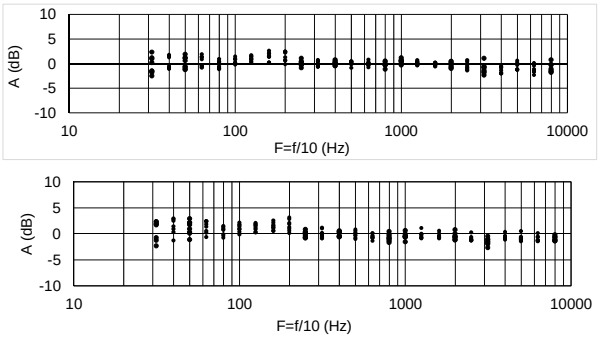

FIGURE V. THE RATIO, $A=I_{LEXP}/I_{LEST}$, BETWEEN THE EXPERIMENTALLY MEASURED INSERTION LOSSES, I_{LEXP}, AND VALUES, I_{LEST}, ESTIMATED FROM (6) AS A FUNCTION OF THE TRAFFIC FREQUENCY F=F/10 FOR ALL EXPERIMENTS CONDUCTED. IN EACH GRAPH EIGHT POINTS AT EACH 1/3 OCTAVE CENTRAL FREQUENCY SHOW THE RESULTS OF MEASUREMENTS AT EIGHT DIFFERENT SOURCE-RECEIVER ANGLES.

Using (6), (7), (8), the single number insertion loss rating, N, (or barrier efficiency) for the traffic barrier can be calculated as (e.g., [8])

$$N(dB) = 10Log_{10}\frac{\sum_{i=n}^{m}10^{0.1S(F_i)}}{\sum_{i=n}^{m}10^{0.1S(F_i)}/10^{0.1IL(F_i)}} \tag{9}$$

where n and m are the lowest and highest values for the 1/3 Octave band center frequencies F_i of practical interest. Thus, the number of parameters in (4) is reduced to three

$$IL(F,R,\theta_S,\theta_M) \Rightarrow N(R,\theta_S,\theta_M) \tag{10}$$

and the data on N, as obtained from the results of all experiments, are summarized in Figure 6, which may be interpreted as the directivity diagram for the function N in (10). Values of N are plotted as functions of the microphone angle, θM, for different sound source angles, θS and distances from the traffic barrier top, R.

In all cases the single number insertion loss ratings, N, increase monotonically and significantly (up to 10 dB) with the increase of the angles of measurements. In contrast, the effect of the distance change on N is small (in average about 2 dB) and may be neglected compare to the effect of the angles changes. This rather unexpected result is in line with the experiments [9] and conclusion that the acoustic efficiency of the edge device is a function of the angles of the source and receiver and independent of their radii.

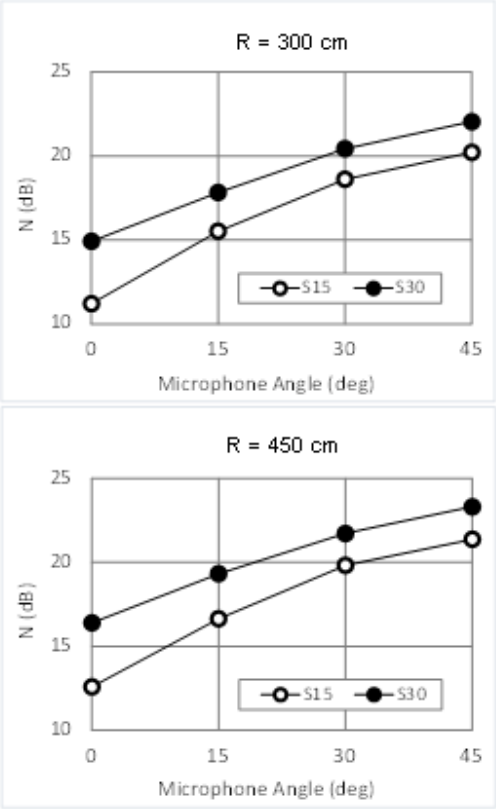

FIGURE VI. DIRECTIVITY DIAGRAMS FOR THE SINGLE NUMBER INSERTION LOSS RATING N AS FUNCTION OF THE MICROPHONE ANGLE, Θ_M, FOR DIFFERENT SOURCE ANGLES, Θ_S (GIVEN IN THE LEGEND) AND TRAFFIC BARRIER TOP DISTANCES, R.

IV. Conclusions

Scaled experiments with straight top traffic noise barriers were conducted. The frequency spectrums of free and diffracted signals were calculated from the sound pressure signals for different source-receiver positions and the insertion loss spectral functions were estimated. The results obtained were rescaled to traffic barriers and for the typical traffic noise spectrum the single number insertion loss ratings were calculated for different source-receiver positions and the directivity diagrams derived. The methodology developed was successfully used for barriers with different top geometries, including T-, L-shape, jagged, etc., "unpublished" [2].

Acknowledgment

P.W. thanks the International School of Engineering, Chulalongkorn University for support of his summer visit to the University of Notre Dame.

References

[1] S.M. Fard, N. Kessissoglou, S.M. Samuels, "A review of road traffic barriers for low frequency noise",. Proceedings of Meetings on Acoustics, 19, 040081, 2013.

[2] S.I. Voropayev, H.J.S. Fernando, "Optimum geometries of noise barriers: scaled experiments", 2015, unpublished.

[3] P.A. Menounoua, "A correction to Maekawa's curve for the insertion loss behind barriers", J. Acoust. Soc. Am., 110 (4), 1828-1838, 2001.

[4] Z. Maekawa, "Noise reduction by screens",. Applied Acoustics, 1, 157–173, 1968.

[5] U.J. Kurze, G.S. Anderson, "Sound attenuation by barriers", Applied Acoustics, 4, 35–53, 1971.

[6] C. Couvreur, "Implementation of a 1/3 octave filter bank in matlab", 1998, unpublished. See also: http://citeseerx.ist.psu.edu/viewdoc/download;jsessionid=BB66616AC1B80CC69EC2D214A83EF58A?doi=10.1.1.57.5728&rep=rep1&type=pdf

[7] T. Ishizuka, K. Fujiwara, "Performance of noise barriers with various edge shapes and acoustical conditions", *Applied Acoustics,* 65 (2), 125-141, 2004.

[8] Garaia, P. Guidorzi, "European methodology for testing the airborne sound insulation characteristics of noise barriers in situ: Experimental verification and comparison with laboratory data", J. Acoust. Soc. Am., 108 (3), Pt. 1, 1054-1067, 2000.

[9] T. Okubo, K. Yamamoto,. "Procedures for determining the acoustic efficiency of edge-modified noise barriers", Applied Acoustics 68, 797–819, 2007.